

Epigenetic Inactivation of *TMS1/ASC* in Ovarian Cancer

Katsuhiko Terasawa,¹ Satoru Sagae,¹
Minoru Toyota,^{2,3,4} Kuniko Tsukada,¹
Kazuhiro Ogi,² Ayumi Satoh,³ Hiroaki Mita,²
Kohzoh Imai,³ Takashi Tokino,² and
Ryuichi Kudo¹

Departments of ¹Obstetrics and Gynecology and ²Molecular Biology and ³First Department of Internal Medicine, Sapporo Medical University, Sapporo, Japan and ⁴PRESTO, JST, Kawaguchi, Japan

ABSTRACT

Purpose: The purpose of this work was to explore the role of epigenetic inactivation of apoptotic pathways in ovarian cancer by examining the DNA methylation and expression status of four proapoptotic genes in primary ovarian cancers and cancer cell lines and to correlate those findings with the clinicopathological features of ovarian cancer patients.

Experimental Design: Genomic DNA was isolated from 15 ovarian cancer cell lines, 80 primary ovarian cancer specimens, and 4 normal ovary specimens using phenol-chloroform extraction. The methylation status of the DNA was evaluated using combined bisulfite restriction analysis, gene expression was evaluated using reverse transcription-PCR, and histone acetylation was evaluated using chromatin immunoprecipitation.

Results: Of the four proapoptotic genes studied, expression of *TMS1/ASC* was absent in six ovarian cancer cell lines. Dense methylation of the 5' region of *TMS1/ASC* was detected in cells not expressing *TMS1/ASC*. Treating methylated cells with 5-aza-deoxycytidine restored gene expression, confirming the role of methylation in silencing the gene. Chromatin immunoprecipitation revealed histone to be deacetylated in cells not expressing *TMS1/ASC*, indicating that histone deacetylation is also involved in silencing *TMS1/ASC*. Aberrant methylation of *TMS1/ASC* was detected in 15 of 80 ovarian cancer tissues (19%) but in none of the normal ovary specimens. Aberrant methylation of *TMS1/ASC* was

observed significantly more often in clear cell-type ovarian cancers than in other tumor types ($P < 0.0001$).

Conclusions: Methylation-mediated silencing of *TMS1/ASC* confers a survival advantage to tumor cells by enabling them to escape apoptosis. The role for aberrant methylation in human ovarian tumorigenesis may be particularly important for ovarian cancers with the clear cell phenotype.

INTRODUCTION

Ovarian cancer is the most deadly of gynecological malignancies, with an overall 5-year survival rate of <30% (1). In large part, this is because the disease usually presents at an advanced stage because there are no overt symptoms at early stages. In addition, ovarian cancers are morphologically and biologically heterogeneous and associated with distinct genetic alterations (2, 3). For example, ovarian cancers of the serous type often show mutations of p53 (4), whereas ovarian cancers of the mucinous type frequently show K-ras mutations (5), and those of the endometrioid type show mutations of β -catenin (6). Little is known about genetic alterations in clear cell-type ovarian cancer.

Epigenetic alterations, such as aberrant methylation of the CpG island in the promoter region, are also associated with the silencing of tumor suppressor genes in human cancers (7, 8). Methylation-mediated gene silencing contributes to malignant progression by inactivating genes involved in tumor suppression, such as those involved in DNA repair and suppressing genomic instability and metastasis. Aberrant methylation likely also contributes to human tumorigenesis by conferring resistance to cell death signals by silencing genes that promote apoptosis (9, 10). In ovarian cancer, aberrant methylation of such cancer-associated genes as *p16INK4A* (11), *RASSF1A* (12), *BRCA1* (13), and *hMLH1* (14) has been reported. The importance of epigenetic alteration of proapoptotic genes in ovarian cancer is largely unexplored, however (15–17).

In the present study, therefore, we examined the methylation status of four proapoptotic genes previously shown to be inactivated by DNA methylation in various types of human neoplasia (9, 18–20). Death-associated protein kinase (DAPK) is a calmodulin-regulated serine/threonine protein kinase involved in diverse apoptosis pathways and in tumor suppression (9, 21). APAF1 is a cell death effector that acts with cytochrome *c* and caspase (CASP) 9 to mediate p53-dependent apoptosis (18). *TMS1/ASC* is a member of the CASP recruitment domain family of proapoptotic mediators and also acts in concert with CASP9 to recruit other activators downstream in this cascade (19). The *TMS1/ASC* gene was originally identified as a target of methylation-induced silencing using cell lines that overexpress DNA methyltransferase 1 (DNMT1). In another critical pathway mediating cell death via death receptors, CASP8 acts as a key apoptotic enzyme by serving as an “initiator CASP”; moreover, CASP8 was recently shown to be silenced by aberrant methylation (20, 22). However, because the 5' region of *CASP8* does not contain a typical CpG island, the relevance of methylation to

Received 6/19/03; revised 12/9/03; accepted 12/10/03.

Grant support: Grant-in-Aid for Scientific Research on Priority Areas from the Ministry of Education, Culture, Sports, Science, and Technology (M. Toyota, K. Imai, and T. Tokino).

The costs of publication of this article were defrayed in part by the payment of page charges. This article must therefore be hereby marked *advertisement* in accordance with 18 U.S.C. Section 1734 solely to indicate this fact.

Note: Dr. Toyota is a Kurozumi Scientific Foundation scholar and Dr. A. Satoh is a research fellow from the Japanese Society for the Promotion of Science.

Requests for reprints: Katsuhiko Terasawa, Department of Obstetrics and Gynecology, South-1 West-16, Chuo-ku, Sapporo 060-8543, Hokkaido, Japan. Phone: 81-11-611-2111, ext. 3368; Fax: 81-11-614-0860; E-mail: kterasaw@sapmed.ac.jp.

Table 1 Primer sequences for TMS1 analysis

		Annealing [°C (cycles)]	Size, enzyme
RT-PCR^a			
TMS1	F: 5'-CGCCGAGGAGCTCAAGAAGTTCA-3' F: 5'-GTACAGAGCATCCAGCAGCCACTCA-3'	60 (35)	364
DAP-K	F: 5'-AACGTGAACATCAAGAACCGAGAA-3' R: 5'-CTGGCTCCCATCAGACAGAGATAC-3'	60 (3), 58 (4), 56 (5), 54 (23)	398
APAF1	F: 5'-ATGAGAGTTTTTCCAGAGGCTTC-3' F: 5'-TTGAGGTAGTACTCCAGCGATTG-3'	60 (35)	403
CASP8	F: 5'-CAGGCTTGTCAGGGGATAACTAC-3' F: 5'-CAAACAAAATAGCACCATCAATCAGA-3'	60 (35)	386
COBRA			
TMS1-set A	F: 5'-GGGGAGTYGGGAGATTAGAGTG-3' R: 5'-AATTCTCCAACRCATCCAAAATAAC-3'	58 (3), 56 (4), 54 (5), 52 (26)	166 <i>TaqI/TaiI</i>
TMS1-set B	F: 5'-TAGGGATAGGTTTTATATTTTGGTTG-3' R: 5'-ACCCRCACCTAATACTACTCA-3'	58 (3), 56 (4), 54 (5), 52 (26)	175 <i>BstUI</i>
DAPK-set A	F: 5'-GTGGGAAGTAGAGAAAGTGGATAGA-3' R: 5'-ACCTCCAAAATACTAAAATTACAAAC-3'	60 (3), 58 (4), 56 (5), 54 (26)	190 <i>TaiI</i>
DAPK-set B ^b	F: 5'-TAGATTTTGTGTYGTTGYGAGTTGT-3' R: 5'-ATCCCCATTAACCRCTACC-3'	55 (3), 53 (4), 51 (5), 49 (26)	157 <i>BstUI</i>
DAPK-set C	F: 5'-TAAAAGGATTGGAGATTGATGTATG-3' R: 5'-TACCCCTTACCTACCAAATTC-3'	55 (3), 53 (4), 51 (5), 49 (26)	188 <i>MboI</i>
ChIP			
TMS1	F: 5'-GAGTCGGGAGACCAGAGTGGGA-3' F: 5'-ACAGCAGCTTCAGCTTGAACCTCTTG-3'	60 (40)	205

^a RT-PCR, reverse transcription-PCR; DAPK, death-associated protein kinase; ChIP, chromatin immunoprecipitation; CASP, caspase.

^b Primers were designed based on the reverse strand Y = C or T, R = G or A.

its silencing remains unclear (22). Here, we have shown that *TMS1/ASC* is inactivated by DNA methylation and histone deacetylation in ovarian cancers. In particular, there was a strong correlation between methylation of *TMS1/ASC* and clear cell-type tumors. These findings shed new light on the molecular basis of this morphological type and could contribute to the development of more specific and effective treatments for ovarian cancer, especially clear cell carcinoma.

MATERIALS AND METHODS

Cell Lines and Specimens. Eight ovarian cancer cell lines (SKOV-3, OVCAR-3, PA-1, Caov-3, TOV112D, TOV21G, SW626, and OV-90) were obtained from the American Type Culture Collection (Manassas, VA); seven others (MH, KURA, AMOC2, MCAS, KF, KFr, and HTBOA) were described previously (23, 24). One cervical cancer cell line (OMC-1) was also examined (25). All cell lines were cultured in RPMI 1640 (Life Technologies, Inc., Rockville, MD) supplemented with 10% fetal bovine serum and incubated under a 5% CO₂ atmosphere at 37°C. Two cell lines that showed aberrant methylation and diminished gene expression were treated with the indicated concentration of a methyltransferase inhibitor, 5-aza-deoxycytidine (5-aza-dC), for 96 h and/or a histone deacetylase inhibitor, trichostatin A, for 24 h. The cells were then harvested, and total RNA was extracted with Isogen (Nippongene, Tokyo, Japan). Four samples of normal ovarian tissue and 80 ovarian cancer specimens were obtained from Sapporo Medical University Hospital at surgery and stored at -80°C. In accordance with institutional guidelines (26), all patients gave informed consent before collection of the specimens.

Reverse Transcription-PCR. Expression of *TMS1/ASC*, *DAPK*, *CASP8*, and *APAF1* was analyzed by reverse transcrip-

tion-PCR. Total RNA was extracted from cell lines using Trizol (Life Technologies, Inc.) according to the manufacturer's instructions. The reverse transcription reaction was performed on 2 µg of total RNA using a SuperScript II First-Strand Synthesis system (Invitrogen) with random primer. PCR was carried out in solution containing 1× PCR buffer (TaKaRa), 200 µM each deoxynucleotide triphosphate, 2.5 pmol of each primer, 1 unit of ExTaq polymerase (TaKaRa), and 5% (v/v) DMSO. The oligonucleotide sequences and PCR parameters used are shown in Table 1. The housekeeping gene *GAPDH* served as an internal control to confirm the success of the reverse transcription reaction. The PCR products were subjected to 2.5% agarose gel electrophoresis.

Combined Bisulfite Restriction Analysis. Genomic DNA was isolated from the cell lines and primary tissue samples (cancerous and normal) using the phenol-chloroform method and then treated with sodium bisulfite as described previously (27). Briefly, 2 µg of DNA were denatured for 10 min at 37°C in 2 M NaOH, after which 30 µl of 10 mM hydroquinone (Sigma Chemical Co) and 520 µl of 3 M sodium bisulfite were added. The mixture was then incubated for 16 h at 50°C, and the modified DNA was purified using a Wizard DNA Purification System (Promega, Madison, WI). After treating the DNA with NaOH a second time, the resultant DNA precipitate was resuspended in 20 µl of 10 mM Tris-HCl-1 mM EDTA buffer and stored at -80°C until use.

The methylation status of *TMS1/ASC* and *DAPK* was examined using combined bisulfite restriction analysis, a semi-quantitative bisulfite-PCR analysis (28). Primers were designed so that both methylated and unmethylated DNA would be amplified equally. PCR was carried out in a 50-µl volume containing 1× PCR buffer [67 mM Tris-HCl (pH 8.8), 16.6 mM

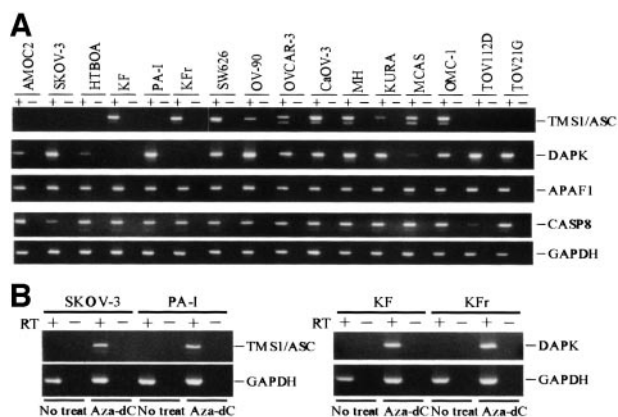


Fig. 1 A, reverse transcription-PCR analysis of expression of proapoptotic genes in ovarian cancer cell lines. Controls consist of carrying out PCR reactions without reverse transcription (–) and amplification of *GAPDH* to assess the integrity of the cDNA. Genes examined are shown on the right. B, restoration of *TMS1/ASC* expression by treatment with 5-aza-deoxycytidine. Reverse transcription-PCR was carried out with RNA extracted from cell lines before (No treat) or after (Aza-dC) incubation of cells with 1 μ M 5-aza-deoxycytidine for 72 h.

(NH_4)₂SO₄, 6.7 mM MgCl₂, and 10 mM β -mercaptoethanol], 0.25 mM deoxynucleotide triphosphate mixture, 0.5 μ M each primer, and 1.0 unit of Hot Start Ex-Taq polymerase (TaKaRa). The oligonucleotide sequences and PCR parameters used for bisulfite-PCR are shown in Table 1.

Bisulfite Sequencing. For bisulfite sequencing, 2 μ l of bisulfite-modified DNA were amplified by PCR using primers TMS1GM1-F and TMS1GM1-R. The amplified products were then cloned into pCR4.0 vector using a TOPO-TA cloning kit (Invitrogen), and at least five clones were sequenced for each cell line analyzed. The plasmid DNA was purified with QIAprep Spin Mini Prep Kit (Qiagen) and then sequenced using a Big Dye Terminator Cycle Sequencing Ready Reaction Kit (Applied Biosystems) with an ABI PRISM 3100 Genetic Analyzer (Applied Biosystems).

Immunofluorescence. Cells were either mock treated or treated with 2.0 μ M 5-aza-dC for 72 h and then fixed in acetone/methanol. D086-3, a monoclonal antibody against human TMS1/ASC developed by Masumoto *et al.* (29), was used as a primary antibody (MBL, Nagoya, Japan). Alexa 488 antimouse IgG antibody (Cosmo Bio, Tokyo, Japan) was used as the second antibody. Finally, the nucleus was stained with Vectashield with 4',6-diamidino-2-phenylindole (Vector Laboratories, Inc., Burlingame, CA), and the cells were examined under a fluorescence microscope (Olympus, Tokyo, Japan).

Chromatin Immunoprecipitation. Chromatin immunoprecipitation was carried out as described previously (30). Briefly, cells were incubated in 1% formaldehyde for 10 min at 37°C. The nuclei were then collected, sonicated to yield fragments ranging in size from 300 to 2000 bp, and immunoprecipitated with anti-histone H3 antibody (Upstate Biotechnology). This antibody specifically recognizes the diacetylated lysine residues (lysines 9 and 14) of histone H3. The chromatin was recovered using protein A-Sepharose. PCR was then carried out in 50 μ l of solution containing 1 μ l of chromatin DNA, 2.5

pmol of each primer, and 25 μ l of SYBR green PCR mixture (Applied Biosystems). The primers used are shown in Table 1. The PCR cycling protocol consisted of 1 cycle at 95°C for 5 min and 40 cycles at 95°C for 30 s and 60°C for 1 min. Fluorescent signals were detected using an ABI 7000 Prism 7000 (Applied Biosystems), and the accumulation of PCR product was measured in real time as the increase in SYBR green fluorescence. Data were analyzed using ABI Prism 7000 SDS Software (Applied Biosystems). Standard curves relating initial template copy number to fluorescence and amplification cycle were generated using the amplified PCR product as a template and used to calculate the DNA copy number in each sample. Ratios of the intensities of the *TMS1/ASC* and *GAPDH* signals were used as a relative measure of the level of *TMS1/ASC* expression in each specimen.

Statistical Analysis. The statistical analysis was carried out using StatView software (SAS Institute Inc., Cary, NC). Fisher's exact test (two-sided) was used to determine the association between TMS1/ASC methylation and clinicopathological features. Values of $P < 0.05$ were considered significant. Overall survival time was defined as the period between the diagnosis of ovarian cancer and the time of death. Differences between survival curves were analyzed using the log-rank test.

RESULTS

We initially examined the expression status of four proapoptotic genes (*TMS1/ASC*, *DAPK*, *APAF1*, and *CASP8*) previously shown to be epigenetically inactivated in human tumors (9, 10, 18–20) using cDNA from 15 ovarian cancer cell lines and 1 cervical cancer cell line (Fig. 1A). Of the four genes studied, *TMS1/ASC* expression was lost in six cell lines (AMOC2, SKOV-3, HTBOA, PA-1, TOV112D, and TOV21G) and diminished in two cell lines (OVCAR-3 and KURA), and expression of *DAPK* was lost in two cell lines (KF and KFr). Expression of *APAF1* and *CASP8*, by contrast, was readily detectable in all 16 cell lines studied. Epigenetic silencing mediated by DNA methylation was responsible for blocking expression of *TMS1/ASC* and *DAPK*, an observation confirmed by the finding that treating the affected cells with a methyltransferase inhibitor (5-aza-dC) restored expression of both (Fig. 1B).

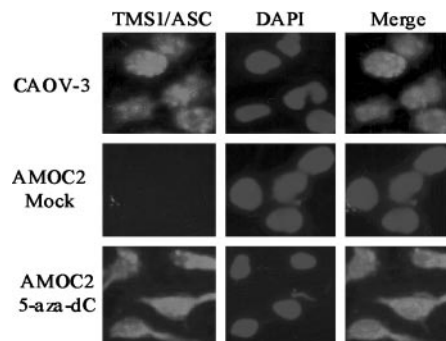


Fig. 2 Immunofluorescence analysis of expression of TMS1/ASC protein in ovarian cancer cell lines. Shown are Caov-3 cells (an unmethylated cell line; top panel), AMOC2 cells (a methylated cell line; middle panel), and AMOC2 cells treated with 5-aza-deoxycytidine (bottom panel).

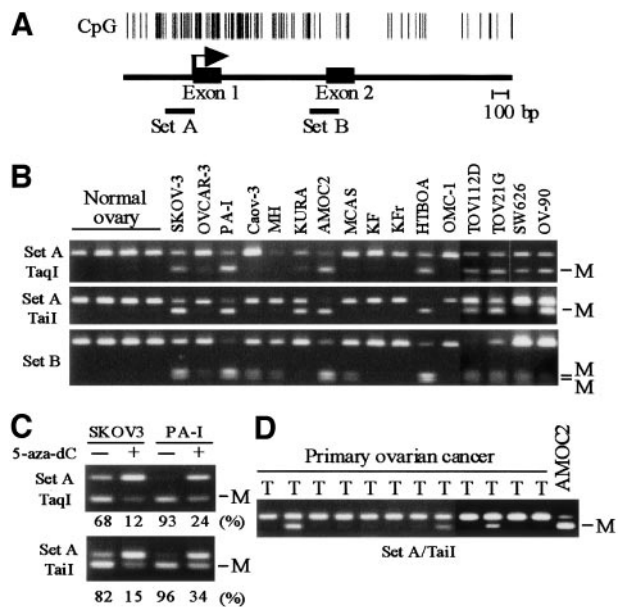


Fig. 3 Analysis of the methylation of the 5' CpG island of *TMS1/ASC*. **A**, CpG sites are shown as vertical bars; exons are indicated by solid boxes on the solid line. The regions analyzed are indicated by the shorter lines below. **B**, representative results of a combined bisulfite restriction analysis of 5' CpG island carried out with a panel of normal ovarian tissues and ovarian cell lines. The methylation status of the three indicated regions of the *TMS1/ASC* CpG island was evaluated by bisulfite-PCR using the appropriate primers. PCR products were digested with restriction enzymes that cleave CpG sites retained after bisulfite treatment because of methylation. M, methylated alleles. The regions and restriction enzymes used are shown on the left. **C**, methylation analysis of *TMS1/ASC* after treatment with a methyltransferase inhibitor, 5-aza-deoxycytidine. SKOV-3 and PA-I cells were treated with 1 μM 5-aza-deoxycytidine for 96 h and harvested. Primer set and restriction enzymes used are shown on the left. Percentages of methylated alleles are shown below the column. M, methylated alleles. **D**, the results of combined bisulfite restriction analysis of the 12 primary ovarian cancer tissues (T) showing aberrant methylation of *TMS1/ASC*. AMOC2 cells served as a positive control for aberrant methylation.

Moreover, immunohistochemical analysis confirmed that *TMS1/ASC* protein was not expressed in cells in which the gene was silenced (Fig. 2) and that expression of the protein was also restored by treatment with 5-aza-dC (Fig. 2).

TMS1/ASC and *DAPK* contain CpG islands that span about 2 kb. To examine in more detail how DNA methylation silences these genes, bisulfite-PCR analysis using primer sets that cover the entire CpG islands of the genes was carried out, followed by restriction digestion (Figs. 3A and 4A). Aberrant methylation of the region around the transcription start site of *TMS1/ASC* was detected in 9 of 16 cell lines (56%) but in none of the 4 normal ovarian tissue specimens (Fig. 3B). Methylation of exon 2 was detected in some cell lines in which expression of *TMS1/ASC* was lost or diminished, although five cell lines that expressed *TMS1/ASC* also showed methylation of exon 2. The fact that demethylation of the 5' region of *TMS1/ASC* was observed after treatment with 5-aza-dC is suggestive of the role played by methylation in the gene silencing (Fig. 3C). Among the primary ovarian cancers, aberrant methylation of *TMS1/ASC* was detected in 15 of 80 (19%) cases (Fig. 3D).

Dense methylation of the region around the 5' transcription start site, 5' CpG island, of *DAPK* was detected in 2 of 16 cell lines (13%) that did not express the gene (Fig. 4B). In contrast, methylation of *Alu* was detected in all cell lines studied, as well as in the four normal ovarian tissue specimens. Methylation of exon 2 was detected in 7 of 16 (44%) cell lines, including 5 cell lines that expressed the gene and 2 cell lines that did not. Apparently, only methylation of the 5' region of the transcription start site, not of *Alu* or exon 2, correlated with loss of expression. None of the 80 primary cancer specimens showed methylation of the 5' CpG island of *DAPK*, indicating it to be a rare event in primary ovarian tumors (Fig. 4C).

We confirmed by bisulfite DNA sequencing that the methylation detected by combined bisulfite restriction analysis reflected the overall methylation level of the region analyzed (Fig. 5). In three cell lines (KURA, SKOV-3, and PA-1) shown by bisulfite-PCR to be densely methylated, almost 90% of the CpG dinucleotides analyzed were methylated. By contrast, the normal ovarian tissue and two cell lines (KF and MCAS) that did not show methylation by bisulfite-PCR were unmethylated at the majority of CpG dinucleotides analyzed.

It was shown recently that deacetylation of histone is also involved in methylation-dependent gene silencing (7, 10, 31). Consistent with those findings, we found that in the methylated SKOV-3 cell line, 5-aza-dC and trichostatin A acted synergistically to restore *TMS1/ASC* expression (Fig. 6A). When we then carried out chromatin immunoprecipitation analysis using an anti-acetylated histone H3 antibody to determine the acetylation status of histone in the *TMS1/ASC* promoter region, we found that methylated cell lines not expressing *TMS1/ASC* (AMOC2,

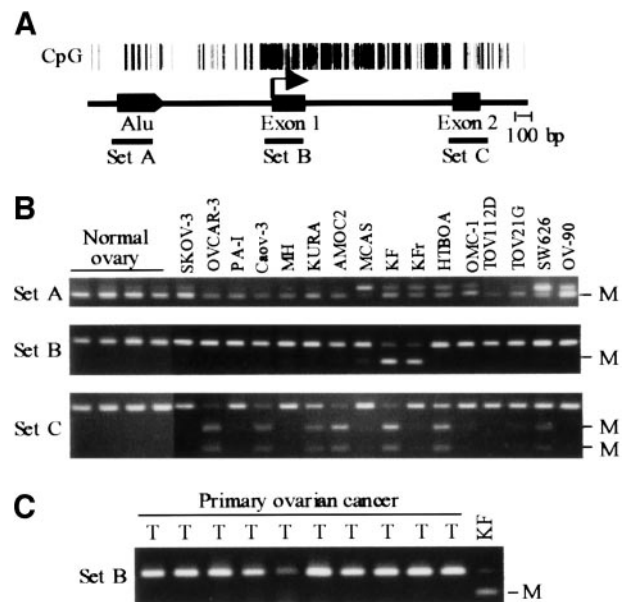


Fig. 4 Methylation analysis of the 5' CpG island of *DAPK*. **A**, CpG island of *DAPK*; CpG sites are shown as vertical bars. Areas analyzed are indicated by solid bars. **B**, bisulfite-PCR analysis of *DAPK* in ovarian cancer cell lines. The regions analyzed are shown on the left. M, methylated allele. **C**, bisulfite-PCR analysis of *DAPK* in primary ovarian cancers. KF cells served as a positive control for methylation.

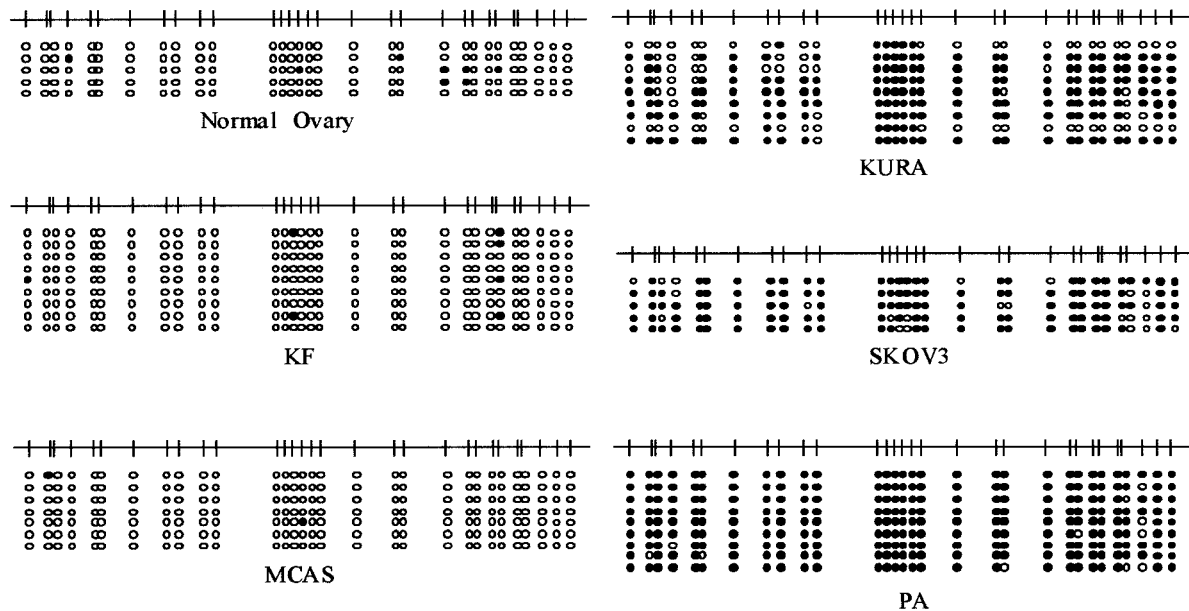


Fig. 5 Bisulfite sequencing of the region around the *TMS1/ASC* transcription start site. Methylation status of individual cloned DNA fragments from five ovarian cell lines and a normal ovarian tissue specimen is shown. Each row represents one sequenced allele. Each circle represents a CpG dinucleotide: ●, methylated CpG sites; and ○, unmethylated CpG sites.

SKOV-3, and HTBOA) showed lower levels of histone acetylation than unmethylated cell lines (KF and MCAS; Fig. 6B).

Finally, we examined the clinicopathological features of ovarian cancers with or without *TMS1/ASC* methylation (Table 2). Aberrant methylation of *TMS1/ASC* was detected in 3 of 23 (13.0%) serous tumors, 1 of 16 (6.3%) endometrioid tumors, 9 of 13 (69.2%) clear cell tumors, no mucinous tumors, and 1 of 5 (20.0%) undifferentiated carcinomas. There was a significant correlation between the clear cell phenotype and *TMS1/ASC* methylation ($P < 0.0001$), but no significant association was seen with any other clinicopathological feature (patient age, the International Federation of Gynecology and Obstetrics [FIGO] clinical stage, and pathological grade). There was also no correlation between the patients' prognoses and the *TMS1/ASC* methylation status (data not shown).

DISCUSSION

Little is known about the changes in proapoptotic genes in ovarian cancers. *TMS1/ASC* is a novel proapoptotic gene previously identified as a target of DNA methylation in breast cancer (19), and we have shown here that aberrant methylation of the 5' region of *TMS1/ASC* is well correlated with loss of expression in ovarian cancer. Notably, decreasing *TMS1/ASC* expression reduces sensitivity to chemotherapeutic drugs (29); *TMS1/ASC* contains a CASP recruitment domain and plays a role in CASP-mediated apoptosis induced by inflammation and chemotherapeutic drugs (32, 33). By enabling them to escape apoptosis, methylation-mediated silencing of *TMS1/ASC* would be expected to contribute to a survival advantage for tumor cells, which supports a role for aberrant methylation in human ovarian tumorigenesis (31, 33).

Methylation of *DAPK* also has been reported in several

tumors, including B-cell malignancy and lung, bladder, colorectal, and gastric cancers (9, 10, 21, 34). We found *DAPK* to be methylated in several ovarian cancer cell lines but in 0 of 80 primary ovarian cancers studied, suggesting that it is a rare event in primary ovarian cancers, and another study showed 2 of 23 (9%) cases of methylation in primary ovarian cancers (35). However, methylation of *DAPK* has been associated with metastasis (34), which suggests that it may be a more common feature of metastatic ovarian cancer. Two cell lines, KF and KFr, did not express *DAPK* as a result of DNA methylation. These cells were originally established from serous cystadenocarcinoma cell lines and are relatively resistant to chemotherapeutic drugs (24, 36). It is thus plausible that epigenetic inactivation of *DAPK* provides cancer cells with the ability to escape apoptosis triggered by the *DAPK* signaling pathway. Obviously, further study will be necessary to determine whether methylation of *DAPK* plays a role in the progression of ovarian cancer *in vivo* or whether it is a cell line-specific event.

We examined several regions of CpG islands to identify aberrant methylation of the *TMS1/ASC* and *DAPK* promoters. Analysis of the *TMS1/ASC* CpG island showed that methylation of the region around the transcription start site, but not the edge of island, is important for gene silencing. Indeed, methylation of the edge of the CpG island was detected in virtually all cell lines tested, regardless of gene expression. We found no age-related methylation of the region around the *TMS1/ASC* transcription start site in normal ovarian tissues from patients.

Of particular interest to us was the finding that methylation of *TMS1/ASC* was associated with the clear cell type of ovarian cancer. The morphological heterogeneity of ovarian cancer clearly contributes to the difficulty of defining the molecular events associated with its development and prognosis. Four

major types of primary ovarian adenocarcinomas have been identified on the basis of morphological criteria: serous; mucinous; endometrioid; and clear cell. Of these, clear cell carcinoma has a particularly unfavorable prognosis and is classified as a high-grade neoplasm in clinical practice. In the present study, aberrant methylation of *TMS1/ASC* was detected in 69% of clear cell carcinomas, which is a significantly higher frequency than was seen in the other histological types (serous, 13%; mucinous, 0%; endometrioid, 6.3%; undifferentiated, 20%). Thus, inactivation of *TMS1/ASC* may play a key role in tumorigenesis of ovarian cancers with a specific etiology and showing the clear cell phenotype.

Evidence suggests that the various histological types of ovarian cancer represent distinct disease entities, and that patterns of gene expression in ovarian cancer reflect both morphology and biological behavior. In fact, ovarian cancer with the clear cell phenotype has a distinctive pattern of gene expression that distinguishes it from other ovarian cancers with poor prognoses (37). For instance, almost all clear cell cancers are resistant to platinum agents, which are key chemotherapeutic agents used in the treatment of ovarian cancer (38). It may be that inactivation of the apoptotic pathway associated with *TMS1/ASC* and *CASP9* contributes to this chemoresistance and to the other biological features of clear cell cancer. Indeed, the prognosis of patients with cancers having the clear cell phenotype are poor, even when the disease is detected at an early stage, and the cancers frequently recur after adjuvant chemotherapy (38). Further study will be necessary to more definitively characterize

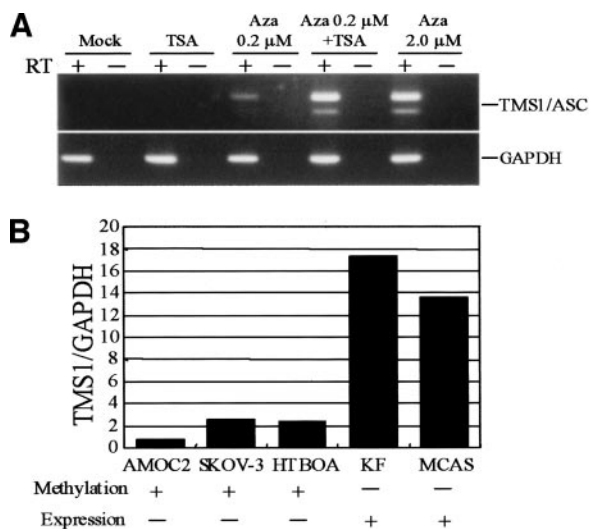


Fig. 6 Role of histone deacetylation in silencing *TMS1/ASC* in ovarian cancer cells. **A**, SKOV-3 cells were treated with 5-azadeoxycytidine (5-aza-dC) and trichostatin A and harvested, after which reverse transcription-PCR was carried out using the cDNA prepared from the cells. The cells were mock treated or treated with 300 nM trichostatin A, 0.2 μM 5-aza-dC, 300 nM trichostatin A + 0.2 μM 5-aza-dC, or 2.0 μM 5-aza-dC. **B**, quantitative analysis of histone acetylation. Chromatin immunoprecipitation analysis was carried out using DNA precipitated with anti-acetylated histone H3 antibody; the bars show the levels of histone acetylation determined by real-time PCR normalized to the *GAPDH* signal. The cell line of interest was indicated below the panel.

Table 2 Patient characteristics and *TMS1* methylation status

Variable	TMS1 methylation		
	+	-	%
FIGO ^a stage			
I	9	13	40.9
II	0	3	0
III	5	34	12.8
V	1	4	20.0
Histological type			
Serous	3	20	13.0
Endometrioid	1	15	6.0
Mucinous	0	6	0
Clear cell	9	4	69.0 ^b
Undifferentiated	1	4	20.0
Others	1	6	14.3

^a FIGO, the International Federation of Gynecology and Obstetrics.

^b Clear cell is significantly different from other types by Fisher's exact test ($P < 0.0001$).

clear cell ovarian cancer. In that regard, methylation analysis may contribute to the development of diagnostic markers to predict sensitivity to chemotherapeutic drugs; moreover, because inhibitors of DNA methylation and histone deacetylation act synergistically to induce expression of *TMS1/ASC*, these drugs may be useful for restoring apoptotic signaling pathways and sensitizing cancer cells to chemotherapeutic agents.

In conclusion, methylation-mediated silencing of *TMS1/ASC* confers a survival advantage to tumor cells by enabling them to escape apoptosis and may thus be a useful target for therapies aimed at treating ovarian cancers resistant to conventional chemotherapy. The role for aberrant methylation in human ovarian tumorigenesis may be particularly important for ovarian cancers with the clear cell phenotype.

ACKNOWLEDGMENTS

We thank Dr. William F. Goldman for editing the manuscript.

REFERENCES

- Landis SH, Murray T, Bolden S, Wingo PA. Cancer statistics, 1999. *CA-Cancer J Clin* 1999;49:8-31.
- Feeley KM, Wells M. Precursor lesions of ovarian epithelial malignancy. *Histopathology* 2001;38:87-95.
- Aunoble B, Sanches R, Didier E, Bignon YJ. Major oncogenes and tumor suppressor genes involved in epithelial ovarian cancer (review). *Int J Oncol* 2000;16:567-76.
- Kupryjanczyk J, Thor AD, Beauchamp R, et al. p53 gene mutations and protein accumulation in human ovarian cancer. *Proc Natl Acad Sci USA* 1993;90:4961-5.
- Enomoto T, Weghorst CM, Inoue M, Tanizawa O, Rice JM. K-ras activation occurs frequently in mucinous adenocarcinomas and rarely in other common epithelial tumors of the human ovary. *Am J Pathol* 1991;139:777-85.
- Sagae S, Kobayashi K, Nishioka Y, et al. Mutational analysis of β-catenin gene in Japanese ovarian carcinomas: frequent mutations in endometrioid carcinomas. *Jpn J Cancer Res* 1999;90:510-5.
- Baylin SB, Esteller M, Rountree MR, et al. Aberrant patterns of DNA methylation, chromatin formation and gene expression in cancer. *Hum Mol Genet* 2001;10:687-92.
- Jones PA. The DNA methylation paradox. *Trends Genet* 1999;15:34-7.

9. Katzenellenbogen RA, Baylin SB, Herman JG. Hypermethylation of the DAP-kinase CpG island is a common alteration in B-cell malignancies. *Blood* 1999;93:4347–53.
10. Satoh A, Toyota M, Itoh F, et al. DNA methylation and histone deacetylation associated with silencing DAP kinase gene expression in colorectal and gastric cancers. *Br J Cancer* 2002;86:1817–23.
11. McCluskey LL, Chen C, Delgadillo E, et al. Differences in p16 gene methylation and expression in benign and malignant ovarian tumors. *Gynecol Oncol* 1999;72:87–92.
12. Yoon JH, Dammann R, Pfeifer GP. Hypermethylation of the CpG island of the RASSF1A gene in ovarian and renal cell carcinomas. *Int J Cancer* 2001;94:212–7.
13. Esteller M, Silva JM, Dominguez G, et al. Promoter hypermethylation and BRCA1 inactivation in sporadic breast and ovarian tumors. *J Natl Cancer Inst (Bethesda)* 2000;92:564–9.
14. Strathdee G, MacKean MJ, Illand M, Brown R. A role for methylation of the hMLH1 promoter in loss of hMLH1 expression and drug resistance in ovarian cancer. *Oncogene* 1999;18:2335–41.
15. Strathdee G, Appleton K, Illand M, et al. Primary ovarian carcinomas display multiple methylator phenotypes involving known tumor suppressor genes. *Am J Pathol* 2001;158:1121–7.
16. Wei SH, Chen CM, Strathdee G, et al. Methylation microarray analysis of late-stage ovarian carcinomas distinguishes progression-free survival in patients and identifies candidate epigenetic markers. *Clin Cancer Res* 2002;8:2246–52.
17. Rathi A, Virmani AK, Schorge JO, et al. Methylation profiles of sporadic ovarian tumors and nonmalignant ovaries from high-risk women. *Clin Cancer Res* 2002;8:3324–31.
18. Fu WN, Bertoni F, Kelsey SM, et al. Role of DNA methylation in the suppression of Apaf-1 protein in human leukaemia. *Oncogene* 2003;22:451–5.
19. Conway KE, McConnell BB, Bowring CE, et al. TMS1, a novel proapoptotic caspase recruitment domain protein, is a target of methylation-induced gene silencing in human breast cancers. *Cancer Res* 2000;60:6236–42.
20. Teitz T, Wei T, Valentine MB, et al. Caspase 8 is deleted or silenced preferentially in childhood neuroblastomas with amplification of MYCN. *Nat Med* 2000;6:529–35.
21. Esteller M, Sanchez-Cespedes M, Rosell R, et al. Detection of aberrant promoter hypermethylation of tumor suppressor genes in serum DNA from non-small cell lung cancer patients. *Cancer Res* 1999;59:67–70.
22. Banelli B, Casciano I, Croce M, et al. Expression and methylation of CASP8 in neuroblastoma: identification of a promoter region. *Nat Med* 2002;8:1333–1335; author reply, 1335.
23. Ishiwata I, Ishiguro T, Ishiwata C, Soma M, Ishikawa H. Establishment and characterization of a human ovarian endodermal sinus tumor cell line-producing specific type of α -fetoprotein subfraction. *Gynecol Oncol* 1986;25:281–93.
24. Kikuchi Y, Miyauchi M, Kizawa I, Oomori K, Kato K. Establishment of a cisplatin-resistant human ovarian cancer cell line. *J Natl Cancer Inst (Bethesda)* 1986;77:1181–5.
25. Ueda M, Ueki M, Yamada T, et al. Scatchard analysis of EGF receptor and effects of EGF on growth and TA-4 production of newly established uterine cervical cancer cell line (OMC-1). *Hum Cell* 1989;2:401–10.
26. Ishioka S, Sagae S, Terasawa K, et al. Comparison of the usefulness between a new universal grading system for epithelial ovarian cancer and the FIGO grading system. *Gynecol Oncol* 2003;89:447–52.
27. Ogi K, Toyota M, Ohe-Toyota M, et al. Aberrant methylation of multiple genes and clinicopathological features in oral squamous cell carcinoma. *Clin Cancer Res* 2002;8:3164–71.
28. Xiong Z, Laird PW. COBRA: a sensitive and quantitative DNA methylation assay. *Nucleic Acids Res* 1997;25:2532–4.
29. Masumoto J, Taniguchi S, Ayukawa K, et al. ASC, a novel 22-kDa protein, aggregates during apoptosis of human promyelocytic leukemia HL-60 cells. *J Biol Chem* 1999;274:33835–8.
30. Magdinier F, Wolffe AP. Selective association of the methyl-CpG binding protein MBD2 with the silent p14/p16 locus in human neoplasia. *Proc Natl Acad Sci USA* 2001;98:4990–5.
31. Stimson KM, Vertino PM. Methylation-mediated silencing of TMS1/ASC is accompanied by histone hypoacetylation and CpG island-localized changes in chromatin architecture. *J Biol Chem* 2002;277:4951–8.
32. Shiohara M, Taniguchi S, Masumoto J, et al. ASC, which is composed of a PYD and a CARD, is up-regulated by inflammation and apoptosis in human neutrophils. *Biochem Biophys Res Commun* 2002;293:1314–8.
33. McConnell BB, Vertino PM. Activation of a caspase-9-mediated apoptotic pathway by subcellular redistribution of the novel caspase recruitment domain protein TMS1. *Cancer Res* 2000;60:6243–7.
34. Tang X, Khuri FR, Lee JJ, et al. Hypermethylation of the death-associated protein (DAP) kinase promoter and aggressiveness in stage I non-small-cell lung cancer. *J Natl Cancer Inst (Bethesda)* 2000;92:1511–6.
35. Esteller M, Corn PG, Baylin SB, Herman JG. A gene hypermethylation profile of human cancer. *Cancer Res* 2001;61:3225–9.
36. Kikuchi Y, Iwano I, Kato K. Effects of calmodulin antagonists on human ovarian cancer cell proliferation in vitro. *Biochem Biophys Res Commun* 1984;123:385–92.
37. Schwartz DR, Kardias SL, Shedden KA, et al. Gene expression in ovarian cancer reflects both morphology and biological behavior, distinguishing clear cell from other poor-prognosis ovarian carcinomas. *Cancer Res* 2002;62:4722–9.
38. Sugiyama T, Kamura T, Kigawa J, et al. Clinical characteristics of clear cell carcinoma of the ovary: a distinct histologic type with poor prognosis and resistance to platinum-based chemotherapy. *Cancer (Phila.)* 2000;88:2584–9.